Assessing Changes in Enriched Maize Flour Formulations After Extrusion by Means of FTIR, XRD, and Chemometric Analysis

Mario Cueto, Abel Farroni, Silvio D. Rodríguez, Regine Schoenlechner, Gerhard Schleining & María del Pilar Buera

Food and Bioprocess Technology
An International Journal

ISSN 1935-5130

Food Bioprocess Technol
DOI 10.1007/s11947-018-2113-6

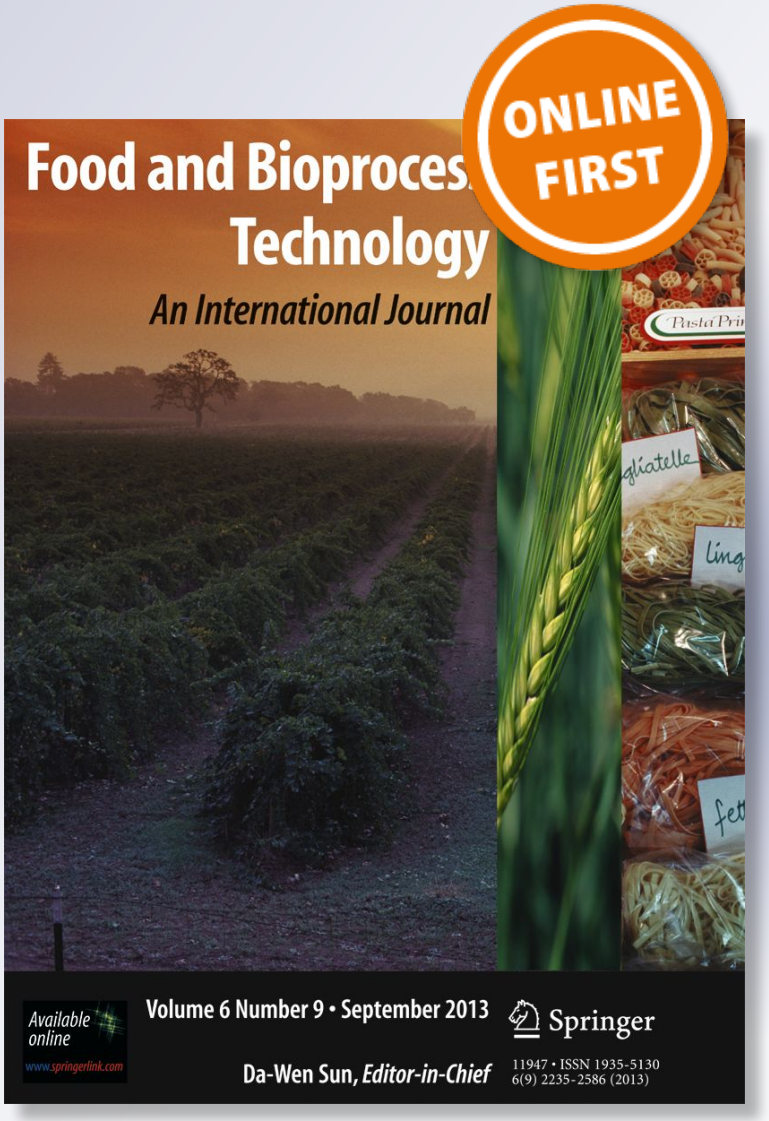

Springer

Food and Bioprocess Technology
https://doi.org/10.1007/s11947-018-2113-6

ORIGINAL PAPER

Assessing Changes in Enriched Maize Flour Formulations After Extrusion by Means of FTIR, XRD, and Chemometric Analysis

Mario Cueto[1] · Abel Farroni[2] · Silvio D. Rodríguez[3] · Regine Schoenlechner[4] · Gerhard Schleining[4] · María del Pilar Buera[1]

Received: 5 July 2017 / Accepted: 10 May 2018

Abstract
Spectral analysis employing multivariate techniques was employed to differentiate plain maize flours from formulations containing maize with added milled chia or quinoa seeds for producing cereal breakfast extrudates. The physicochemical changes of the enriched formulations due to processing stages and formulation were evaluated by using FTIR and *chemometric* analysis, which allowed a rapid and non-destructive discrimination between sample processing and compositional aspects. Specific IR frequencies were selected which provided highest sample discrimination. Selected IR absorbance relationships at those specific wavenumbers were useful to track changes promoted by extrusion for carbohydrates, proteins, and lipids. The complexes between amylose and lipids, that takes place during extrusion, underwent distinctive changes as confirmed by XRD. The crystallinity loss, after extrusion (with an average value of 50%), shows evidence of amylose-lipid complexes formation of type E_h and V_h. Correlations between the textural behavior, composition, and selected FTIR indices were obtained.

Keywords Extrudates · FTIR · XRD · Maize flour · Texture

Introduction

Many of the existing ready-to-eat extruded snacks are relatively high in sugar and salt, thus being regarded as energy dense but nutritionally poor foods (Brennan et al. 2013). Maize is frequently used as main ingredient. However, it is possible to manipulate the nutritional status of these extruded snacks by incorporating sources of proteins and unsaturated lipids from alternative crops (Sharma et al. 2012), such as quinoa and chia seeds, of widely recognized high nutritional value. Quinoa (*Chenopodium quinoa Willd*) is a pseudocereal that has served as a chief food source for ancestral Andean populations (Nascimento et al. 2014). Chia (*Salvia hispanica*) is an oilseed that has been cultivated in Mexico for thousands of years. Both quinoa and chia seeds have a higher protein content than cereal grains, quinoa being particularly rich in essential amino acids (Ruales and Nair 1992). Chia seeds have a high proportion of poly-unsaturated fatty acids and a very low starch content in comparison to cereal grains (Valdivia-López and Tecante 2015).

Conventional extrusion is one of the main processes employed to obtain breakfast cereals. It is a continuous high-temperature and short time cooking process, which combines heating, pressure, and high shear forces at relatively low water contents, in comparison with traditional cereal cooking. Thus, extensive physical and chemical modification occurs and special molecular interactions are developed. Extrusion of cereal flours results in the destruction of starch granules, degradation of the starch polymer chains, denaturation and aggregation of proteins, formation of starch–lipid and protein–lipid complexes, and protein–protein cross-linking. Starch is considered

✉ Mario Cueto
mariocueto@gmail.com

[1] Facultad de Ciencias Exactas y Naturales, Departamento de Industrias, Universidad de Buenos Aires, Intendente Güiraldes 2160, C1428EGA Buenos Aires, Argentina

[2] Laboratorio de Calidad de Alimentos, Suelos y Aguas, INTA Pergamino, Av. Frondizi (Ruta 32) km. 4,5 Pergamino CC 31, B2700WAA Buenos Aires, Argentina

[3] Facultad de Ciencias Exactas y Naturales, Departamento de Biodiversidad y Biología Experimental, Universidad de Buenos Aires, Intendente Güiraldes 2160, C1428EGA Buenos Aires, Argentina

[4] Department of Food Sciences and Technology, BOKU-University of Natural Resources and Life Sciences, Gregor-Mendel-Straße 33, 1180 Wien, Austria

Published online: 07 June 2018

the most important component for the production of highly acceptable extruded snack foods (Rampersad et al. 2003). In the extrudates, starch forms a continuous amorphous phase, while the proteins are present as a discontinuous phase (Hermansson 1988). Chemical transformation of macromolecular components also occurs during extrusion processing which modifies the functional and digestive characteristics of the extrudates (Singh et al. 2007; Jyothi et al. 2009).

During extrusion cooking, the native structure of amylose is partially disrupted, and new crystalline networks, corresponding to the amylose-lipid complex, are formed (Merayo et al. 2011). The presence and type of amylose-lipid complexes have an important influence on structure, texture, and other functional properties of the puffed extrudates (Bhatnagar and Hanna 1997; Desrumaux et al. 1999). For example, it plays an important role in increasing shelf life of extruded products by providing protection against lipid oxidation Ilo et al. 2000.

The combination of maize with other flours, as a common strategy for improving the physical, chemical, and nutritional quality of extruded products, as mentioned above, strongly influence the expansion degree, breaking strength, hardness, density, and other quality parameters of extrudates (Ramos Diaz et al. 2013; Cueto et al. 2015). However, the full evaluation of their impact in cereal changes during processing and final product characteristics is a difficult task by means of traditional technologies.

Fourier transform infrared spectra (FTIR) employing total attenuated reflectance (ATR) has being widely used to evaluate product composition and to identify chemical modifications induced by different processing methods. It is, in fact, a non-destructive technique, which also avoids complex preparation procedures. This technique was used by Shrestha et al. (2010) to study changes in long- and short-range molecular order caused by extrusion procedure in high-amylose maize starch. FTIR spectroscopy has allowed the confirmation of the formation of hydrogen bonds between blend components (Jiménez-Elizondo et al. 2009) and also changes in crystalline/amorphous fractions of maize starch (Liu et al. 2011) or amaranth subjected to ball-milling treatment (Roa et al. 2014a). The spectral analysis can be coupled to multivariate techniques (also known as chemometric methods), allowing analysis of information from the spectra by means of differences and similarities, and to discriminate and group samples of selected characteristics according to different physical or chemical properties (Van den Berg et al. 2013).

Starch processed by extrusion cooking has also been studied employing the X-ray diffraction technique (XRD) to identify crystal structures and regular molecular arrangements present in native and processed starch (Ottenhof et al. 2005).

The aim of this study was to evaluate the impact of flour blend formulation on the macromolecular changes of corn-based extrudates enriched with quinoa and chia by employing non-destructive FTIR, XRD, and chemometric methods.

Materials and Methods

Materials

Whole corn flour, quinoa, and chia seeds were purchased from a local market. All other reagents used were of analytical grade and used as received.

Preparation of the Formulations and Extrusion Process

Flour formulations for extrusion were prepared by mixing corn flour with chia or quinoa flours. As moisture content is determinant of extrusion performance, all grains were equilibrated to 14% water content on wet basis (w.b.). When it was needed, small quantities of water were added and grains were mixed and equilibrated in a controlled chamber (75% relative humidity, 25 °C). This process was repeated until all grains reached 14% w.b. humidity. Water content was measured gravimetrically by drying the milled samples (passing 0.420-mm mesh) during 4 h at 130 °C under forced air current until constant weight (± 0.0002 g); all samples were run in triplicate. For sample preparation, quinoa seeds were grinded in a laboratory mill (Grindomix GM300- Retsch, Germany) prior to mixing. Chia seeds were also grinded employing small quantities of liquid N_2 to minimize oxidation of lipids. Three different samples were blended at room temperature in a mechanical mixer for 1 h. Mixtures, consisting of plain maize (M), maize with 20% of quinoa (M + Q), and maize with 5% of chia (M + C), were prepared before the extrusion process. Protein and ash content of flour blends in this study in percent dry basis (% d.b.) were proteins: M: 8.9 ± 0.3, M + Q: 11.5 ± 0.4, M + C: 10.2 ± 0.4 and ash: M: 1.3 ± 0.1, M + Q: 2.0 ± 0.2, M + C: 1.5 ± 0.1. Protein value was obtained by Kjeldhal (AOAC 992.23), using a conversion factor of 6.25, and ashes following AOAC (923.03).

As the fat content of the flour mix is an important factor in extrusion processes, samples were formulated so that the amount of fat was lower than 5%, to avoid problems with the extrusion process due to high lipid content. Singh et al. (2007) pointed out that the torque of the extruder decreases by the effect of lipids that increase the slip within the barrel and thus less pressure is developed resulting in a less expanded product.

The samples were extruded using a conical extruder (Cincinnati Milacron CM45-F, Austria) equipped with a twin screw and using counter-rotating feeding. The screw geometry was length 1000 mm, diameter from 90 to 45 mm, channel depth 8.5 mm, calender gap 0.5 mm, and flight gap 0.2 mm. A screw configuration with five conveying sections and three drossel zones was used and a 4.5-mm circular die was fitted in the die plate. The feeding was fixed at 45 kg/h and screw speed at 69 RPM. The barrel heating section was set at 50, 80,

100, and 150 °C, respectively, and the operating torque was set at 80%. After extrusion, the samples were left to cool at room temperature for 12 h and stored in sealed polyethylene bags for further analyses.

Before FTIR and XRD analysis, samples were grinded (M-11basic IKA-Werke GmbH & Co. KG, Staufen, Germany) until the entire sample passed throw a 75-μm mesh screen.

Fourier Transform Infrared Spectra

The samples from the different formulations were scanned in a Fourier Transform Infrared spectrometer (FTIR Spectrum 400, Perkin Elmer Inc., Shelton CT, USA). A few milligrams of each sample were placed over a diamond/ZnSe crystal with one reflectance and an incident angle of 45° in the attenuated total reflectance (ATR) accessory (PIKE Technologies, Inc. Madison, WI, USA) and scanned from 600 to 4000/cm with a resolution of 4/cm until 64 scan were accumulated at 25 °C. Three replicates of each sample were scanned and the resultant spectra corrected by using the same base baseline with the Spectrum software (Perkin Elmer Inc.). Additionally, spectra were normalized and transformed considering the intensity in absorbance units. Since the diamond/ZnSe crystal showed absorbance in the 1800–2500/cm region, this spectra interval was not considered in further analyses.

X-ray diffractometry

X-ray diffraction patterns of the samples were recorded in a Phillips Xpert MPD (PANanalytical, B.V., Almelo, Netherlands) using Cu Kα radiation. The operating conditions were 0.1542-nm radiation wavelength, 40 kV voltage and a 35 mA current. Diffractograms were scanned over the 2θ range of 6–30°, with a scan rate of 0.03°/2 s. The percentage of crystallinity was calculated for each diffractogram with a method described by Roa et al. (2014a), and using the following equation:

$$\%\text{crystallinity} = \frac{A_c}{(A_{\text{am}} + A_c)} \times (100) \quad (1)$$

where A_c is the area calculated for the crystalline fraction and A_{am} is the area calculated for the amorphous fraction. The percentage of crystallinity values reported were the average of three diffractograms from each sample.

Physical Variables

The expansion rate (ER) was calculated as the relationship between the average sample diameter (measured with a digital caliper in five samples) and the die diameter (4.5 mm) (Alvarez-Martinez et al. 1988). Bulk density (ρ_b) was calculated using a 5-L graduated cylinder filled to the top and weighted (five replicates). True density (ρ_t) was measured after grinding the samples using the volume displacement method (Yan et al. 2008) employing toluene as solvent (triplicates of each sample were run). Porosity was estimated as a relation between both densities (Bisharat et al. 2013) according to Eq. (2)

$$\varepsilon = 1 - (\rho b)/(\rho t) \quad (2)$$

Mechanical Properties

A Kramer shear test was performed with a texture analyzer TAXT plus (Stable Microsystems, UK) using a 5-bladed HDP/KS5 with an acoustic envelope detector for sound measurement. Twenty repetitions of each sample were measured. The tests were carried at a blade speed of 1 mm/s until 3-cm target distance was reached. Trigger force was set to 0.08 N. The microphone was positioned at a 3-cm distance with an angle of 45° to the sample. The amplifier was set to level 4 and the data acquisition rate was 500 points per second. Ten replicates of each sample were analyzed. From the force signal the maximum force (N), distance to maximum force (mm), area (total area obtained upon deformation with the blade going up to 3-cm depth) (N.mm), number of peaks, and linear distance (N/s) were measured. From the acoustic signal, the mean sound peak (dB), acoustic linear distance (dB/s), acoustic area (total area obtained under the sound wave with the blade going up to 3-cm depth) (dB.mm), and number of acoustic peaks were evaluated.

Principal Component Analysis

Principal component analysis (PCA) is a well-known statistical procedure for determining similarities among the objects in a two-way data set (e.g., samples by selected wavelengths). To this end, the relative locations of the samples on the most important principal components in a two- or three-dimensional plot are compared (Jolliffe 2002). Another outcome from the PCA method is the so-called loading matrix, which is composed by the values associated to the most relevant wavelengths for grouping the samples by their similarity. PCA on the covariance matrix were performed using Infostat/p2011 software.

Cluster Analysis (*K-means* Method)

In cluster analysis (CA), a set of objects (similar to PCA) is assigned to a number of groups (i.e., clusters), specified previously by the user, in such a way that samples belonging to the same cluster are more similar to each other than objects belonging to different clusters (Johnson and Wichern 2002).

The outcomes of the analysis are a clusterization vector, which indicates the designation of each sample to a cluster and a goodness of fit value called *average silhouette width* (ASW), which could take values from − 1 to 1, and must be greater than 0.75 for a good assignment of the samples to the clusters (Kaufman and Rousseeuw 1987). *K-means* analysis was performed using the Infostat/p2011 software.

Analysis of Variance

The differences among the means where evaluated using ANOVA with a Tukey post-hoc test, $p < 0.5$ (Infostat/p2011).

Results and Discussion

FTIR Indices and Macromolecular Behavior

Differences in the spectral regions corresponding to vibrations of the main chemical groups of lipid and starch structures could be detected in Fig. 1. These spectral regions were analyzed employing PCA and cluster analysis (CA), after base line correction and normalization of spectra by the 996/cm band (Roa et al. 2014b), comparing each blend formulation against pure maize formulations.

After this analysis, some major regions were found to be the most determinant regarding spectral differences (Table 1). Indexes in bibliography reported many of these regions as main protein, lipids, and carbohydrate regions. Some small differences in wavenumbers (2–5/cm) were found in same cases regarding the informed indexes that could be generated by the local environment of the molecules.

The region of frequencies around 1000–1100/cm is attributed mainly to starch groups. It has been described with absorption maxima at 996/cm (C-O bending of the glycosidic bond), 1014/cm (C-O stretching, C-O-C/C-O bending), and 1039/cm (C-O bending) (Capron et al. 2007). The loading analysis from PCA (Table 1) shows that only the 965/cm (Fig. 1a) and 961/cm (Fig. 1b) wavenumbers appeared as one of the main loadings of PC1. The main bands associated with proteins are generally described with maxima at 1640/cm (C=O stretching and NH bending) and 1540/cm (C-N stretching, C-O stretching, and C-C stretching) and are attributed to amide I and amide II bonds, respectively (Barth 2007; Guzman-Ortiz et al. 2014). In the PCA, these bands were not present as one of the most relevant wavenumbers. This was somehow surprising since extrusion process has been addressed to generate major changes in proteins. Furthermore, the bands at 2922, 2853/cm (symmetric and asymmetric stretching of CH_2) and 1745/cm (stretching of the ester carbonyl group) are associated with bond vibrations originated from the lipids present in the samples (Cremer and Kaletunç 2003; Jiménez-Elizondo et al. 2009). In this region, 2854/cm and 2923/cm showed high loadings for PC1 after Fig. 1a and 2855/cm and 2923/cm for PC1 after Fig. 2b. The 1745/cm appeared with high contributions on the PC2 (Fig. 1a, b).

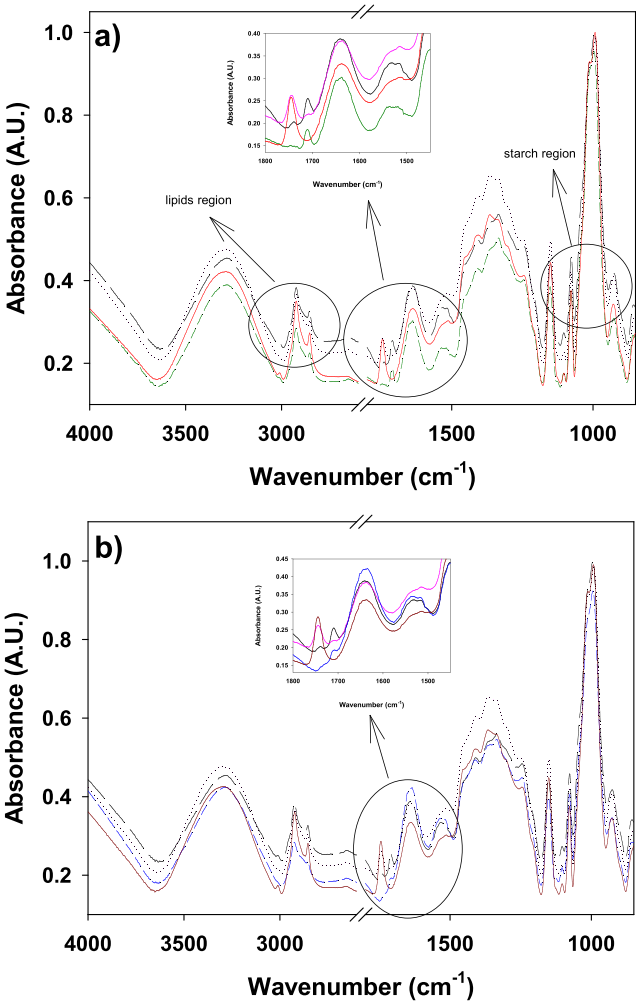

Fig. 1 Absorbance spectra for FTIR-ATR **a** (− −) raw maize, (●●●●) extruded maize, (▬▬) raw maize+Q, (▬▬) extruded maize+Q; **b** (− −) raw maize, (●●●●) extruded maize, (▬▬) raw maize+C, (▬▬) extruded maize+C

Figure 1a, b shows the normalized FTIR spectra of pure maize flour and of the mixture maize/quinoa (M + Q) and maize/chia (M + C) before and after extrusion. One of the main changes in the FTIR spectra during the extrusion process is associated to the disappearance of the band at 1710/cm and the appearance of a band at 1745/cm (after extrusion). This could be related to the ester carbonyl vibration of the lipids interacting with other components (i.e., proteins or carbohydrates) which changes through the extrusion process shifting the signal to higher frequencies. Ester carbonyl absorption bands are sensitive for conformational changes, responsive to polarity changes of their local environments, and are influenced by hydrogen bonding and other interactions (Lewis et

Table 1 Most relevant wavelengths associated to each principal component (cm^{-1})

Samples	Component	Wavenumbers (/cm)							
(Fig. 1a)	PC1	965	913	2854	2923	1515	1225	1119	1446
	PC2	1369	1403	1456	1048	1746	1070	954	1148
(Fig. 1b)	PC1	961	915	2855	2923	1200	1136	1289	1711
	PC2	1745	1369	1068	1398	1049	1457	954	1091

al. 1994). Also, the band with a maximum at 1640/cm (amide I) exhibited a slight broadening after the extrusion, and the same occurred with the band associated to amide II (1540/cm) including a decrease in the intensity of the absorption, attributable to protein denaturation (Guerrero et al. 2014). Such changes related to protein denaturation can promote modifications in the interactions with other macromolecules, with increased accessibility of the peptide bond residues to H-H exchange, which shifts the frequency to about 1450/cm (Mendelsohn et al. 1984; Fabian and Mäntele 2006).

Since the effects of both, process and the composition, were reflected in the resulting spectra, the samples can be differentiated before and after the extrusion. Spectra regions associated with the higher loading factors are shown in Table 1. Figure 2 shows the first two PC comparing M + C (a) and M + Q (b) with maize only. PC1 and PC2 accumulated 92.4% (71.9 PC1; 20.5 PC2) (a) and 97% (80.3 PC1 and 16.7 PC2) (b) of the total variance. In both analyses, it was observed that for the PC1, the main loadings were in the starch (961, 915, 980 to 1150/cm) and lipids (2855, 2923/cm) regions. For the PC2, the highest loadings were in frequencies associated with lipids (1750/cm) and carboxylic groups 1369, 1457/cm.

To be able to quantify the different changes in macromolecules, the peak/band maxima are shown in Table 2, as a ratio of intensities for all the samples extruded and not extruded, following the procedure by Roa et al. (2014b).

The relationship between the absorbance peaks with respect to the 996/cm absorbance values was used to standardize the spectra with difference in intensities, allowing a

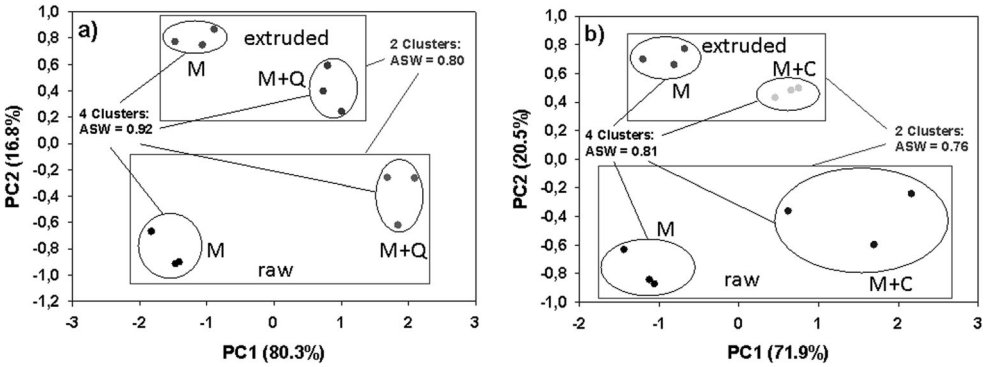

Fig. 2 Cluster analysis for **a** maize (M) and maize+chia (M + C), raw and extruded and **b** maize (M) and maize+quinoa (M + Q), raw and extruded. ASW are shown between formulas and between the set of raw and the extruded samples

Table 2 Indexes calculated form the selected absorbance frequencies of FTIR spectra. Different letters account for statistical differences using ANOVA with Tukey pot hoc test ($p < 0.05$)

Index	Sample					
	M CE	M SE	M + Q CE	M + Q SE	M + C CE	M + C SE
1039/1014	$0.47^{a} \pm 0.01$	$0.52^{c} \pm 0.02$	$0.47^{ab} \pm 0.01$	$0.51^{bc} \pm 0.01$	$0.46^{a} \pm 0.01$	$0.54^{c} \pm 0.02$
996/1014	$1.10^{ab} \pm 0.01$	$1.14^{c} \pm 0.02$	$1.08^{a} \pm 0.02$	$1.08^{a} \pm 0.01$	$1.09^{ab} \pm 0.01$	$1.12^{bc} \pm 0.02$
1640/996	$0.24^{a} \pm 0.01$	$0.23^{a} \pm 0.03$	$0.22^{a} \pm 0.02$	$0.21^{a} \pm 0.01$	$0.22^{a} \pm 0.01$	$0.30^{b} \pm 0.02$
1740/996	$0.07^{c} \pm 0.01$	$-0.03^{a} \pm 0.01$	$0.10^{d} \pm 0.01$	$-0.01^{b} \pm 0.01$	$0.14^{e} \pm 0.01$	$-0.05^{a} \pm 0.01$
1380/1455	$1.25^{a} \pm 0.01$	$1.37^{c} \pm 0.04$	$1.25^{ab} \pm 0.01$	$1.39^{c} \pm 0.02$	$1.23^{a} \pm 0.01$	$1.31^{b} \pm 0.02$
1455/996	$0.41^{d} \pm 0.01$	$0.32^{b} \pm 0.01$	$0.37^{c} \pm 0.02$	$0.28^{a} \pm 0.01$	$0.38^{cd} \pm 0.01$	$0.33^{b} \pm 0.01$
1380/996	$0.51^{d} \pm 0.01$	$0.43^{bc} \pm 0.01$	$0.46^{bc} \pm 0.02$	$0.39^{a} \pm 0.01$	$0.47^{cd} \pm 0.01$	$0.43^{ab} \pm 0.01$
2920/996	$0.201^{b} \pm 0.008$	$0.154^{a} \pm 005$	$0.216^{bc} \pm 004$	$0.14^{a} \pm 0.02$	$0.25^{c} \pm 0.01$	$0.15^{a} \pm 0.02$
2850/996	$0.107^{b} \pm 0.004$	$0.076^{a} \pm 0.003$	$0.119^{bc} \pm 0.004$	$0.07^{a} \pm 0.01$	$0.142^{c} \pm 0.007$	$0.07^{a} \pm 0.01$

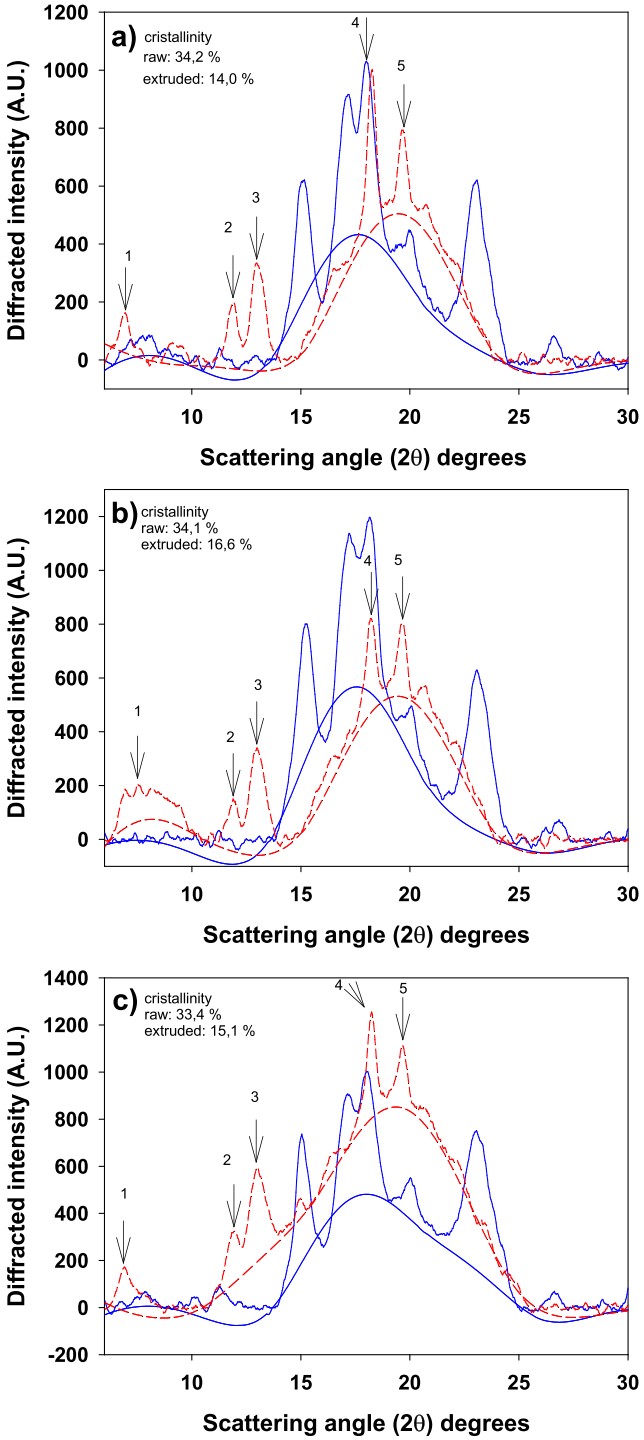

Fig. 3 X-ray diffraction patterns for **a** maize (M), **b** maize+quinoa (M + Q), **c** maize+chia (M + C) blends. Lines correspond to raw (continuous lines) and extruded (dotted lines) samples. In each case, the lower curve corresponds to the amorphous region calculated employing Savitzky and Golay smoothing function (after 50 iterations). Arrows show the new peaks that appeared after processing

quantitative analysis. This peak is chosen because is generally described as the main starch peak, which is the main component of our extruded samples, and because of that remains relatively unchanged through the different spectra.

The 1039/1014 index (ratio between absorbance values at 1039 and 1014/cm) has been previously employed to relate the amorphous and crystalline zones in starch (Sevenou et al. 2002). In our samples, the effect of extrusion can be seen in this index, which changed significantly with the process for M and M + C formulas, indicating a decrease in crystallinity. The 996/1014 index did not show major changes before and after the process. A protein related index, 1640/996, has been previously used as an indicator of protein changes during extrusion (Guerrero et al. 2014). Only M + C showed changes in this index. The ratio 1380/996 was significantly lower and 1455/996 higher for all samples as a consequence of extrusion. These two bands are well defined in a pure dextrin spectrum. The high barrel temperature can damage maize starch structure at molecular, crystalline, and granular levels leading to the re-association of starch molecules, and molecular weight decreases during extrusion processing (Yang et al. 2016). This change could also be favored as a consequence of the mechanical shear and low water content of the system. At the same time, the absorbance ratio 1380/1455 decreased after extrusion and could be indicating an increase in the protonated carboxylic groups compared to the non-protonated ones (Guzman-Ortiz et al. 2014).

The index 1740/996 increased after the process. This change can be associated to the C=O stretching of the lipid carbonyl groups and would increase if more freedom is attained as a consequence of breaking the interactions in lipid-starch complexes. This index was also different between extruded samples. The other two lipid related indices 2920/996 and 2850/996 also increased after extrusion. They have been used to study the starch lipid complex (Flores-Morales et al. 2012) that is affected by extrusion (Thachil et al. 2014).

In general, differences between processed samples were reflected in the indices related to lipids (2920/996 and 2850/996) (Table 2). The other selected indices did not show significant differences among the various sample formulations but did present differences between the raw and extruded samples, underlying the greater influence in the macromolecular behavior of the overall extrusion process for over smaller changes in ingredients formulation.

Starch Crystallinity Through XRD Analysis

In order to further analyze changes in starch crystallinity and complex formation discussed in the previous section, X-ray diffractograms were performed on the raw and extruded samples. Water content of the extruded products was around 8% w.b. (8.46% ± 0.04 for maize extrudates, 8.32% ± 0.06 for the extrudates with quinoa, and 8.2% ± 0.1 for the extrudates with chia). All diffractograms are presented with two broad rounded peaks, corresponding to the starch amorphous regions, and those with sharper peaks corresponding to the crystalline areas (Fig. 3). The crystalline structure was of type A, characteristic

Table 3 Physical, mechanical, and acoustic properties obtained after a Kramer Cell assay

Type of variable	Variable name	Sample		
		Control	Quinoa	Chia
Mechanic	Area	$1957.42^{b} \pm 252.1$	$1286.25^{a} \pm 509.81$	$2552.18^{c} \pm 399.33$
	N° peaks	$653.2^{a} \pm 84.73$	$925^{b} \pm 376.89$	$614.7^{a} \pm 116.58$
	Distance (mm)	$-54.50^{b} \pm 4.47$	$-63.72^{a} \pm 5.20$	$-52.96^{b} \pm 2.7$
	Linear distance	$3280.25^{b} \pm 293.79$	$2169.15^{a} \pm 661.89$	$2254.14^{a} \pm 188.04$
	F max	$147.68^{b} \pm 11.79$	$108.79^{a} \pm 24.86$	$198.28^{b} \pm 18.84$
Acoustic	Area	$1901.25^{b} \pm 36.19$	$1668.52^{a} \pm 194.94$	$1919.98^{c} \pm 46.82$
	Linear distance	$84{,}624.46^{b} \pm 2808.31$	$71{,}110.6^{a} \pm 12{,}975.94$	$86{,}663.52^{b} \pm 7708.44$
	Mean	$63.39^{b} \pm 1.21$	$55.63^{a} \pm 6.5$	$64.01^{b} \pm 1.56$
	N° peaks	$3013.5^{a} \pm 76.09$	$3096^{ab} \pm 223.23$	$3268.3^{b} \pm 127.03$
Physic[1]	Expansion index	$5.39^{b} \pm 0.25$	$5.82^{c} \pm 0.23$	$4.98^{a} \pm 0.36$
	Porosity	$96.30^{a} \pm 0.20$	$96.800^{a} \pm 0.001$	$96.600^{a} \pm 001$
	True density	$1.46^{ab} \pm 0.04$	$1.44^{a} \pm 0.01$	$1.53^{b} \pm 0.01$
	Bulk density	$0.054^{c} \pm 0.001$	$0.046^{a} \pm 0.001$	$0.052^{b} \pm 0.002$

Different letters indicate significant differences were found among the formulations ($p < 0.05$)

[1] Physical properties of the extruded samples were extracted from Cueto et al. (2015)

of maize starch (Jane et al. 1997; Cheetham and Tao 1998; Han et al. 2007), with two main refraction peaks at 2 15° and 23°, and a maximum near 18°. Quinoa starch has been reported to present also type A structure (Atwell et al. 1982; Qian and Kuhn 1999). During extrusion, heating and mechanical shear can disrupt the starch granules, promoting loss in native starch structure (Roa et al. 2014a). As a result, after the process, the three peaks corresponding to 15, 18, and 23° disappeared, indicating a loss of the granular crystallinity (type A). At the same time, the appearance of new peaks at 2.8, 12, and 18.2° (arrows 1, 2, and 3 in Fig. 3) reflected the formation of amylose-lipid complexes with E_h type structures (Mercier et al. 1980; Fan et al. 1996). The peak at 19.8° (arrow 4 in Fig. 3) could correspond to the V_h form (Bhatnagar et al. 1994). This form can be generated at high temperatures, after starch gelatinization. Both types of crystals can appear together after the extrusion process being the E_h variant favored under reduced water availability and higher temperatures (Cairns et al. 1997). In addition, conversion from V to E forms can occur during heating (Le Bail et al. 1999). There is also a new peak at 13–14° (arrow 5 in Fig. 3) which could not be assigned to a particular event.

From the area under the curve, the crystallinity was estimated following the procedure explained by Roa et al. (2014a). After spectra smoothing, crystalline and amorphous areas were calculated, and the percentage of crystallinity was evaluated for all samples, before and after extrusion (Fig. 3), observing changes due to processing. Values for raw samples

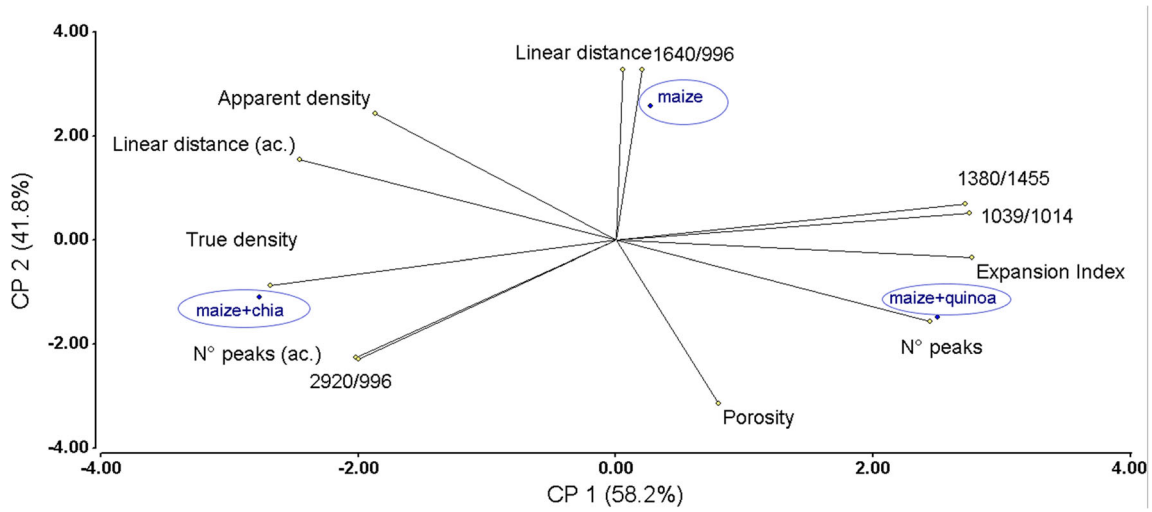

Fig. 4 Biplot of the two principal components obtained including the IR indexes, physical, mechanical, and acoustic properties

were similar to the ones reported for native starch (around 30%) in maize samples (Utrilla-Coello et al. 2014). In addition, Qian and Kuhn (1999) reported a 35% of crystallinity for native quinoa starch, which is also comparable to the values obtained in this work for native samples. After extrusion, all samples showed a loss of 50% of the initial crystallinity, with the remaining crystallinity attributed to the formation of amylose-lipid complexes and that of native starch that has not been transformed. A linear relationship between the percentage of crystallinity by XRD and FTIR indices was evaluated. For the 1039/1014 index, R^2 was 0.91. This result is in concordance to the findings of Roa et al. (2014a) for amaranth starch (native and submitted to ball milling). We also evaluated the XRD correlation with 1740/996 and 1380/1455 indices, showing R^2 of 0.77 and 0.8 respectively.

Relation Between FTIR Indices, Physical, Texture, and Acoustic Variables

In order to reveal the relation between the FTIR indices and the macroscopic behavior of the samples, a PCA was performed. The set of variables included the most representative FTIR indices selected from the present work together with physical variables (bulk density, true density, expansion index, and porosity) and mechanical properties obtained from a compression test performed employing a Kramer cell on the same samples. These variable values were taken from our previous work (Cueto et al. 2015) and listed in Table 3.

The variables presented in Table 3 were examined for linear correlations between them. The ones that showed the highest Pearson coefficients (R^2) were the following: expansion index with 1039/1014 ($R^2 = 0.99$), expansion index with 1380/1455 ($R^2 = 0.95$), porosity with 1640/996 ($R^2 = -0.96$), linear distance with 1640/996 ($R^2 = 1.0$), and number of peaks with 1039/1014 ($R^2 = 0.86$). These relations can also be spotted in the biplot of Fig. 4, where they are situated either together in the diagram (positive coefficients), or in opposites sides of the axis (negative coefficients).

Figure 4 shows the biplot from the two first PC. PC1 and PC2 accounted for the 100% of the variability indicating no information loses in the variable reduction. PC1 was positively correlated to expansion index and number of peaks and negatively correlated to true density and apparent density in a lower extent. In this way, extrudates with good physical properties would have positive values on this ax. In addition, PC1 correlated positively with 1039/1014, 1380/1555, and number of peaks. M + Q sample appeared located at high PC1 values. Exactly opposite, we found the lipids related index (2920/996) and the true and apparent density, with the M + C samples on this side. PC2 correlated positively with linear distance and 1640/996 index and negatively with porosity.

It can be noticed that the chia samples (the one with the highest lipid content), in the lower part of the plot, have the highest value for the lipid related index 2920/996, while the maize sample is found on the upper part, towards higher linear distance values.

The proposed FTIR analysis could be employed as a useful tool to obtain indices that explain the relationships present among the characteristic changes in macromolecules and the physical, texture, and acoustic properties. After the extrusion process, these changes were evidenced through a multivariate aided FTIR analysis, showing that the extracted indices could be helpful to understand more in depth the physical behavior of the final sample.

Conclusion

FTIR in combination with chemometric methods (PCA and CA) were useful for discrimination with a 100% of success of the samples with addition of quinoa or chia in comparison of pure maize samples before and after the extrusion process.

FTIR was also successfully used to differentiate the physicochemical behavior and final products of the different flour blends under extrusion cooking process.

The proposed absorbance relationships at selected wavenumbers were useful in tracking changes promoted by extrusion at molecular level with impact on mechanical properties.

Aided by an exhaustive multivariate study, the most significant differences among spectra of samples with different formulations and from different process stages could be found, which are connected to the behavior of the different macromolecules in the systems.

Starch crystallinity loss after extrusion averaged 50%, showing evidence of amylose-lipid complexes of type Eh and Vh, confirmed by XRD analysis, which data correlated with FTIR selected variables. Macromolecular interactions evidenced trough a multivariate aided FTIR analysis were related to the final physical and textural behavior of the samples.

Acknowledgments M.P.B. and S.D.R. are members of the *CONICET* research staff. A.F. is a member of the Instituto Nacional de Tecnología Agropecuaria (INTA, Pergamino). M.C. is a recipient of a *CONICET* fellowship.

Funding Information This work was supported by Bilateral Cooperation Project MINCYT-BMWF (AU1205.WTZ Project Nr. AR 16/2013.), Agencia Nacional de Promoción Científica y Tecnológica (PICT 2013-1331), Universidad de Buenos Aires (UBACYT 20020130100443BA), and Instituto Nacional de Tecnología Agropecuaria (PNAyVA 1130043).

References

Alvarez-Martinez, L., Kondury, K. P., & Harper, J. M. (1988). A general model for expansion of extruded products. *Journal of Food Science, 53*(2), 609–615.

Atwell, W. A., Patrick, B. M., Johnson, L. A., & Glass, R. W. (1982). Characterization of quinoa starch. *Cereal Chemistry, 60*(1), 9–11.

Barth, A. (2007). Infrared spectroscopy of proteins. *Biochimica et Biophysica Acta, 1767*(9), 1073–1101.

Bhatnagar, S., & Hanna, M. A. (1997). Modification of microstructure of starch extruded with selected lipids. *Starch, 49*(1), 12–20.

Bisharat, G. I., Oikonomopoulou, V. P., Panagiotou, N. M., Krokida, M. K., & Maroulis, Z. B. (2013). Effect of extrusion conditions on the structural properties of corn extrudates enriched with dehydrated vegetables. *Food Research International, 53*(1), 1–14. https://doi.org/10.1016/j.foodres.2013.03.043.

Brennan, M. A., Derbyshire, E., Tiwari, B. K., & Brennan, C. S. (2013). Ready-to-eat snack products: the role of extrusion technology in developing consumer acceptable and nutritious snacks. *International Journal of Food Science and Technology, 48*(5), 893–902.

Cairns, P., Morris, V. J. S. N., & Smith, A. C. (1997). X-ray diffraction studies on extruded maize grits. *Journal of Cereal Science, 26*(2), 223–227.

Capron, I., Robert, P., Colonna, P., Brogly, M., & Planchot, V. (2007). Starch in rubbery and glassy states by FTIR spectroscopy. *Carbohydrate Polymers, 68*(2), 249–259.

Cheetham, N. W. H., & Tao, L. (1998). Variation in crystalline type with amylose content in maize starch granules: an X-ray powder diffraction study. *Carbohydrate Polymers, 36*(4), 277–284.

Cremer, D. R., & Kaletunç, G. (2003). Fourier transform infrared microspectroscopic study of the chemical microstructure of corn and oat flour-based extrudates. *Carbohydrate Polymers, 52*(1), 53–65.

Cueto, M., Porras-Saavedra, J., Farroni, A., Alamilla-Beltrán, L., Schonenlechner, R., Schleining, G., & Buera, P. (2015). Physical and mechanical properties of maize extrudates as affected by the addition of chia and quinoa seeds and antioxidants. *Journal of Food Engineering, 167*, 139–146.

Desrumaux, A., Bouvier, J. M., & Burri, J. (1999). Effect of free fatty acids addition on corn grits extrusion cooking. *Cereal Chemistry, 76*(5), 699–704.

Fabian, H., & Mäntele, W. (2006). Infrared spectroscopy of proteins biochemical applications infrared spectroscopy of proteins. *Handbook of Vibrational Spectroscopy*.

Fan, J., Mitchell, J. R., & Blanshard, J. M. V. (1996). The effect of sugars on the extrusion of maize grits—the role of glass transmission in determining product density and shape. *International Journal of Food Science and Technology, 31*, 51–65.

Flores-Morales, A., Jiménez-Estrada, M., & Mora-Escobedo, R. (2012). Determination of the structural changes by FT-IR, Raman, and CP/MAS 13C NMR spectroscopy on retrograded starch of maize tortillas. *Carbohydrate Polymers, 87*(1), 61–68.

Guerrero, et al. (2014). FTIR characterization of protein-polysaccharide interactions in extruded blends. *Carbohydrate Polymers, 111*, 598–605.

Guzman-Ortiz, F. A., Hernández-Sánchez, H., Yee-Madeira, H., San Martín-Martínez, E., Robles-Ramírez, M. C., Rojas-López, M., Berríos, J. J., & Mora-Escobedo, M. (2014). Physico-chemical, nutritional and infrared spectroscopy evaluation of an optimized soybean/corn flour extrudate. *Journal of Food Science and Technology, 52*(7), 4066–4077.

Han, M., Chang, M., & Kim, M. (2007). Changes in physicochemical properties of rice starch processed by ultra-fine pulverization. *Journal of Applied Biological Chemistry, 50*, 234–238.

Hermansson, A.-M. (1988). Gel structure of food biopolymers. In J. M. V. Blanshard & J. R. Mitchell (Eds.), *Food structure. Its creation and evaluation* (p. 25). London: Butterworths.

Ilo, S., Schoenlechner, R., & Berghofe, E. (2000). Role of lipids in the extrusion cooking processes. *Grasas y Aceites, 51*, 97–110.

Jane, J. L., Wong, K. S., & McPherson, A. E. (1997). Branch-structure difference in starches of A and B-type X-ray patterns revealed by their Naegelidextrins. *Carbohydrate Research, 300*(3), 219–227.

Jiménez-Elizondo, N., Sobral, P. J. A., & Menegalli, F. C. (2009). Development of films based on blends of Amaranthus cruentus flour and polyvinyl alcohol. *Carbohydrate Polymers, 75*(4), 592–598.

Johnson, R. A., & Wichern, D. W. (2002). Applied multivariate statistical analysis. New.

Jolliffe, I. T. (2002). *Principal component. analysis* (2nd ed.). New York: Springer.

Jyothi, A. N., Sheriff, J. T., & Sajeev, M. S. (2009). Physical and functional properties of arrowroot starch extrudates. *Journal of Food Science, 72*, E97–E104.

Kaufman, L., & Rousseeuw, P. J. (1987). Statistical data analysis based on the L1 norm. In Y. Dodge (Ed.), *Clustering by means of medoids* (pp. 405–416). North-Holland: Prentice Hall.

Le Bail, P., Bizot, H., Ollivon, M., Keller, G., Bourgaux, C., & Buléon, A. (1999). Monitoring the crystallization of amylose–lipid complexes during maize starch melting by synchrotron x-ray diffraction. *Biopolymers, 50*(1), 99–110.

Lewis, R. N., McElhaney, R. N., Pohle, W., & Mantsch, H. H. (1994). Components of the carbonyl stretching band in the infrared spectra of hydrated 1,2-diacylglycerolipid bilayers: a reevaluation. *Biophysical Journal, 67*(6), 2367–2375.

Liu, T., Ma, Y., Yu, F., Shi, J., & Xue, S. (2011). The effect of ballmilling treatment on structure and porosity of maiz starch granule. *Innovative Food Science & Emerging Technologies, 12*(4), 586–593.

Mendelsohn, R., Anderle, G., Jaworsky, M., Mantsch, H. H., & Dluhy, R. A. (1984). Fourier transform infrared spectroscopic studies of lipid-protein interaction in native and reconstituted sarcoplasmic reticulum. *Biochimica et Biophysica Acta (BBA) - Biomembranes, 775*(2), 215–224.

Merayo, Y. A., Gonzalez, R. J., Drago, S. R., Torres, R. L., & De Greef, D. M. (2011). Extrusion conditions and Zea mays endosperm hardness affecting gluten-free spaghetti quality. *International Journal of Food Science and Technology, 46*(11), 2321–2328.

Mercier, C., Charbonniere, R., Ggrebaut, J., & de la Gueriviere, J. F. (1980). Formation of arnylose-lipid complexes by twin screw extrusion cooking of manoic starch. *Cereal Chemistry, 57*, 4–9.

Nascimento, A. C., Mota, C., Coelho, I., Gueifão, S., Santos, M., Matos, A. S., Gimenez, A., Lobo, M., Samman, N., & Castanheira, I. (2014). Characterization of nutrient profile of quinoa (Chenopodium quinoa), amaranth (Amaranthuscaudatus), and purple corn (Zeamays L.) consumed in the North of Argentina: Proximates, minerals and trace elements. *Food Chemistry, 148*, 420–426.

Ottenhof, M. A., Hill, S., & Farhat, I. A. (2005). Comparative study of the retrogradation of intermediate water content waxy maize, wheat, and potato starches. *Journal of Agricultural and Food Chemistry, 53*(3), 631–638.

Qian, J., & Kuhn, M. (1999). Characterization of Amaranthus cruentus and *Chenopodium quinoa* starch. *Starch-Stärke, 51*(4), 116–120.

Ramos Diaz, J. M., Kirjoranta, S., Tenitz, S., Penttilä, P. A., Serimaa, R., Lampi, A.-M., & Jouppila, K. (2013). Use of amaranth, quinoa and kañiwa in extruded corn-based snacks. *Journal of Cereal Science, 58*(1), 59–67.

Rampersad, R., Badrie, N., & Comissiong, E. (2003). Physico-chemical and sensory characteristics of flavoured snacks from extruded cassava/pigeonpea flour. *Journal of Food Science, 68*(1), 363–367.

Roa, F. D., Buera, M. P., Tolaba, M., & Acosta, D. F. R. (2014a). Amaranth milling strategies and fraction characterization by FT-IR. *Food and Bioprocess Technology, 7*, 711.

Roa, F. D., Santagapita, P. R., Buera, M. P., & Tolaba, M. P. (2014b). Ball milling of amaranth starch-enriched fraction. Changes on particle size, starch crystallinity, and functionality. *Food and Bioprocess Technology, 7*(9), 2723–2731.

Ruales, J., & Nair, B. (1992). Nutritional quality of the proteins in quinoa (Chenopodium quinoa Willd.) seeds. *Plant Food for Human Nutrition, 42*(1), 1–11.

Sandoval-Oliveros, M., & Paredes-López, O. (2013). Isolation and characterization of proteins from chia seeds (Salvia hispanica L.). *Journal of Agriculture and Food Chemistry., 61*, 193−201.

Sevenou, O., Hill, S. E., Farhat, I. A., & Mitchell, J. R. (2002). Organization of the external region of the starch granule as determined by infrared spectroscopy. *International Journal of Biological Macromolecules, 31*(1-3), 79–85.

Sharma, P., Gujral, H. S., & Singh, B. (2012). Antioxidant activity of barley as affected by extrusion cooking. *Food Chemistry, 131*(4), 1406–1413.

Shrestha, K., Ng, C., Lopez-Rubio, A., Blazek, J., Gilbert, E., & Gidley, M. (2010). Enzyme resistance and structural organization in extruded high amylose maize starch. *Carbohydrate Polymers, 80*(3), 699–710.

Singh, S., Gamlath, S., & Wakeling, L. (2007). Nutritional aspects of food extrusion: a review. *International Journal of Food Science and Technology, 42*(8), 916–929.

Tapia-Blácido D. (2006). Edible films based on amaranth flour and starch. PhD thesis. Department of Food Engineering, Campinas, SP, Brazil.

Thachil, M. T., Chouksey, M. K., & Gudipati, V. (2014). Amylose-lipid complex formation during extrusion cooking: effect of added lipid type and amylose level on corn-based puffed snacks. *International Journal of Food Science and Technology, 49*(2), 309–316.

Utrilla-Coello, R. G., Hernández-Jaimes, C., Carrillo-Navas, H., González, F., Rodríguez, E., Bello-Pérez, L. A., & Alvarez-Ramirez, J. (2014). Acid hydrolysis of native corn starch: morphology, crystallinity, rheological and thermal properties. *Carbohydrate Polymers, 103*(1), 596–602.

Valdivia-López, M. A., & Tecante, A. (2015). Chia (*Salvia hispanica*): a review of native Mexican seed and its nutritional and functional properties. *Advances in Food and Nutrition Research, 75*, 53–75.

Van den Berg, F., Lyndgaard, C. B., Sørensen, K. M., & Engelsen, S. B. (2013). Process analytical technology in the food industry. *Trends in Food Science and Technology, 31*(1), 27–35.

Yan, Z., Sousa-Gallagher, M. J., & Oliveira, F. A. R. (2008). Shrinkage and porosity of banana, pineapple and mango slices during air-drying. *Journal of Food Engineering., 84*(3), 430–440. https://doi.org/10.1016/j.jfoodeng.2007.06.004.

Yang, Q., Yang, Y., Luo, Z., Xiao, Z., Ren, H., Li, D., & Yu, J. (2016). Effects of lecithin addition on the properties of extruded maiz starch. *Journal of Food Processing and Preservation, 40*(1), 20–28. https://doi.org/10.1111/jfpp.12579.